

Electronic Structure of AlO_2 , AlO_2^- , Al_3O_5 , and Al_3O_5^- Clusters

Ana Martínez and Francisco J. Tenorio

Instituto de Investigaciones en Materiales, Universidad Nacional Autónoma de México, Ciudad Universitaria, Circuito Exterior, A. P. 70-360, Delegación de Coyoacán, 04510 México D. F., México

J. V. Ortiz*

Department of Chemistry, Kansas State University, Manhattan, Kansas 66506-3701

Received: July 16, 2001; In Final Form: October 12, 2001

Density functional, quadratic configuration interaction, and electron propagator calculations have yielded structures, isomerization energies, and anion vertical electron detachment energies pertaining to AlO_2 , AlO_2^- , Al_3O_5 , and Al_3O_5^- . These data suffice for an accurate assignment of recent anion photoelectron spectra. Al_3O_5^- has a planar structure with three tricoordinate Al cations, three bridging oxides, and two terminal oxides. Dyson orbitals associated with the lowest electron detachment energies are dominated by p functions on terminal oxygens.

Introduction

Various phases of Al_2O_3 are found in ceramics, minerals, reactive surfaces, and catalytic supports and are generally held to consist of Al trications and O dianions. Reactions between aluminum and oxygen produce a broad array of intermediates, but only some exhibit the bulk stoichiometric ratio. Photoelectron spectra of AlO_n^- and Al_3O_n^- clusters were presented by Wang's group at several photon energies.^{1–3} The AlO_2^- and Al_3O_5^- clusters are especially pertinent to bulk electronic structure, for they conform to the simple electron counts expected for Al_2O_3 .

In this paper, we attempt to assign the most prominent peaks in the photoelectron spectra of AlO_2^- and Al_3O_5^- . Density functional methods suffice for identification of likely structures of the anions and to confirm the similarity of neutral structures in their ground states. After refinement of the anion structures with quadratic configuration interaction methods, electron propagator methods are used to determine vertical electron detachment energies. These results are compared to photoelectron data.

Methods

Density Functional Calculations. All calculations have been carried out using the program GAUSSIAN-98.⁴ Full geometry optimization without symmetry constraints was performed using the hybrid B3LYP density functional (DF)⁵ and the 6-311+G-(2d) basis.⁶ Full geometry optimizations starting from several initial geometries have been performed to locate distinct minima on potential energy surfaces. In search of the global minimum, several multiplicities and initial structures were considered. We cannot exclude the possibility that global minima were missed, but the diversity of initial geometries and spin multiplicities that were examined is sufficient to inspire confidence that the global minimum has been identified. Optimized geometries were verified with frequency calculations.

Electron Propagator Calculations. The most stable anionic structures from DF calculations were reexamined with additional

geometry optimizations at the QCISD level.⁷ 6-311G(d) and 6-311+G(2d) basis sets were used.⁶ Only minor discrepancies between DF and QCISD structures were found.

QCISD geometries were used in subsequent electron propagator⁸ calculations of the vertical electron detachment energies (VEDEs) of the anions. 6-311+G(2df) basis sets were used.⁶

To each VEDE calculated with the electron propagator, there corresponds a Dyson spin-orbital

$$\phi^{\text{Dyson}}(x_1) = \sqrt{N} \int \Psi_{\text{anion}}(x_1, x_2, x_3, \dots, x_N) \Psi_{\text{neutral}}(x_2, x_3, x_4, \dots, x_N) dx_2 dx_3 dx_4 \dots dx_N \quad (1)$$

whose normalization integral equals the pole strength, p , where

$$p = \int |\phi^{\text{Dyson}}(x_1)|^2 dx_1 \quad (2)$$

In the zeroth order electron propagator, ionization energies are given by Koopmans's theorem, Dyson orbitals equal canonical Hartree–Fock (HF) orbitals, and pole strengths equal unity. In the present, correlated calculations, however, Dyson orbitals are linear combinations of HF orbitals, and pole strengths lie between 1 and 0. Since the Dyson orbitals are subject to a nonlocal, energy-dependent potential known as the self-energy, relaxation and correlation corrections to ionization energies and pole strengths are present. Plots of Dyson orbitals are generated with MOLDEN.⁹

The NR2 electron propagator method is used here. This approximation is suitable for calculating the lowest electron detachment energies of closed-shell species.¹⁰ For ionization energies of typical, closed-shell, organic molecules below 20 eV, the average absolute error is less than 0.2 eV. However, for Al_3O_n^- clusters with $n = 1–3$, more refined BD-T1 calculations produced higher ionization energies. The shift factor was approximately 0.3 eV for final states corresponding to oxygen-dominated Dyson orbitals.

Results and Discussion

Density Functional Geometry Optimization. The initial geometries that were used are shown in Figure 1. We tested

* To whom correspondence should be addressed. E-mail: ortiz@ksu.edu.

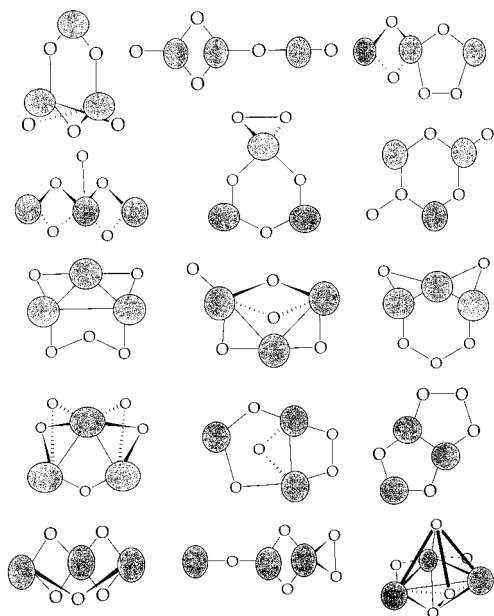


Figure 1. Initial structures in Al_3O_5 and Al_3O_5^- geometry optimizations.

different bond distances and angles for each structure. For neutral and anionic Al_3O_5 , several stationary points on each potential energy surface were found. Figure 2 presents the most stable (neutral and anionic) structures for Al_3O_5 . The most stable anionic structure, for example, was obtained by optimization of the preliminary geometry displayed in the left column and the third row of Figure 1. The next most stable anion followed from the structure in the center of the top row of the same figure.

For Al_3O_5 , there are two stable structures, with an energy difference of 10.0 kcal/mol. The ground state is a nonplanar structure with C_{2v} symmetry. A side view displays the two oxygen bridges that connect the two lowest Al nuclei. For the anionic system, two different spin multiplicities (singlet and triplet) are considered. The ground state is a singlet, and the singlet–triplet splitting is 27.5 kcal/mol. There are two stable singlet structures with an energy difference of 15.5 kcal/mol. The ground state has a planar C_{2v} structure that is similar to that of the second most stable neutral isomer. There is also a nonplanar structure at 20.1 kcal/mol that resembles the lowest neutral isomer. For Al_3O_5 , a three-dimensional structure is preferred over planar ones; for the anionic system, planar structures are more stable than three-dimensional ones.

Ab Initio Results

AlO_2^- . For AlO_2^- , only one structure with $D_{\infty h}$ symmetry need be examined. Structures found in the DF calculations were reoptimized at the QCISD/6-311+G(2d) level. The resulting Al–O bond length is 1.641 Å, in excellent agreement with the DF value, 1.637 Å.

In the photoelectron spectrum of AlO_2^- ,^{1,2} peaks occur at 4.23, 4.88, and 5.08 eV. NR2 results with the 6-311+G(2df) basis at 4.15, 4.80, and 5.00 eV correspond to ${}^2\Pi_g$, ${}^2\Pi_u$, and ${}^2\Sigma_u$ final states, respectively. Pole strengths are 0.88, 0.87, and 0.87 for the three electron detachment energies. Identical results are obtained when the top three virtual orbitals, which correspond to core functions, are omitted from the NR2 calculations.

Dyson orbitals for the three electron detachment energies are dominated by oxygen functions. (See Figure 3.) The 0.03 contours for the π_g Dyson orbital are determined chiefly by

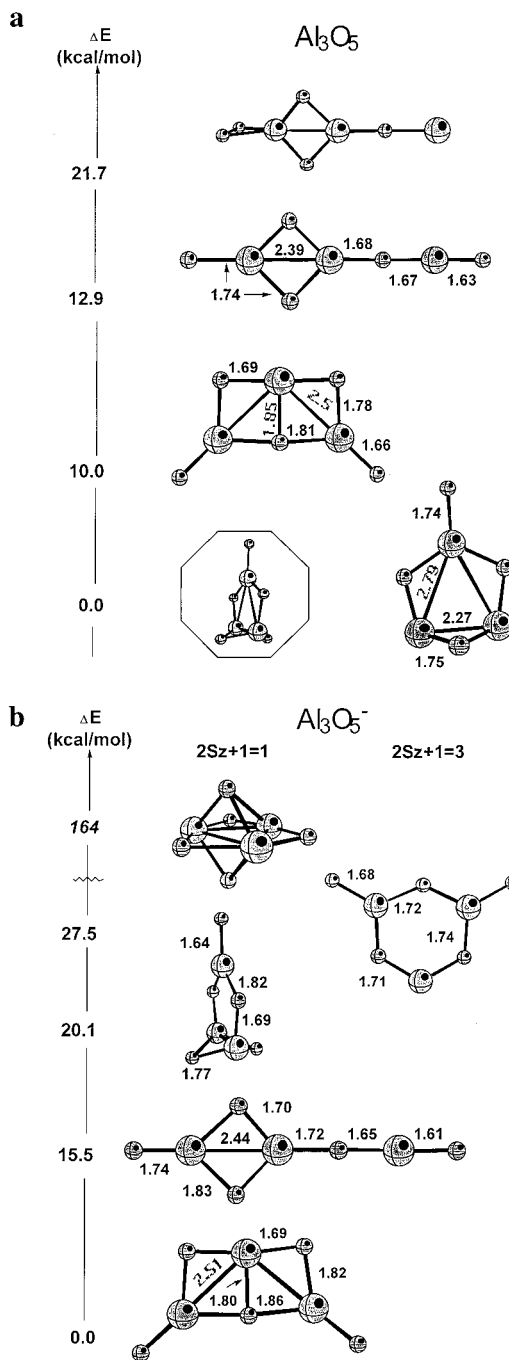


Figure 2. Al_3O_5 (a) and Al_3O_5^- (b) structures and energies.

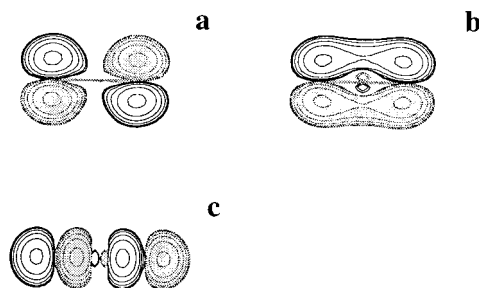


Figure 3. Dyson orbitals for VEDEs of AlO_2^- : (a) ${}^1\Sigma_g \rightarrow {}^2\Pi_g$, (b) ${}^1\Sigma_g \rightarrow {}^2\Pi_u$, (c) ${}^1\Sigma_g \rightarrow {}^2\Sigma_u$.

symmetry considerations. Some delocalization into the neighborhood of the Al nucleus occurs for the π_u and σ_u Dyson orbitals.

TABLE 1: Al_3O_5^- VEDEs (eV)

final state	KT	NR2 ^a	PES ³
$^2\text{B}_2$	6.46	4.97 (0.87)	5.21
$^2\text{A}_1$	6.48	4.99 (0.87)	
$^2\text{B}_1$	6.36	5.10 (0.87)	
$^2\text{A}_2$	6.38	5.13 (0.87)	
$^2\text{B}_2$	7.87	6.18 (0.87)	
$^2\text{A}_1$	7.95	6.29 (0.87)	
$^2\text{B}_1$	10.26	8.66 (0.87)	
$^2\text{A}_1$	10.68	8.76 (0.87)	
$^2\text{A}_2$	10.48	8.99 (0.92)	

^a Pole strengths in parentheses.

Al_3O_5^- . DF calculations clearly establish the planar, C_{2v} structure with three tricoordinate Al ions as the lowest isomer of Al_3O_5^- . QCISD/6-311G(d) optimizations begun from the DF minimum arrive at essentially the same structure; bond lengths are in close agreement with DF values.

NR2 calculations are performed with the 6-311+G(2df) basis. In accord with our results on AlO_2^- , the top eight virtual orbitals are dropped. Results are shown in Table 1. The order of states given by canonical orbital energies via Koopmans's theorem (KT) differs from the sequence predicted by NR2 calculations. Correlation corrections to KT results are large, especially for the higher final states. Pole strengths are between 0.87 and 0.92; shakeup character in these final states has only minor importance. The first six final states are grouped in pairs with similar energies.

In the photoelectron spectrum of Al_3O_5^- , a broad feature begins around 4.9 eV, has a maximum around 5.2 eV, displays shoulders near 5.4 and 5.6 eV, and ends near 5.7 eV.² Information on higher energies is not available due to the frequency of the photon source. A figure of 5.21 eV was given as the vertical ionization energy.

After applying a 0.3 eV shift mentioned above to the first two predicted electron detachment energies of Table 1, there is close agreement between the 5.21 eV figure and the NR2 results. Four final states, $^2\text{B}_2$, $^2\text{A}_1$, $^2\text{B}_1$, and $^2\text{A}_2$ contribute to the broad feature in the photoelectron spectrum. NR2 results predict a separation of only 0.2 eV between the lowest and highest members of this set. Considerable vibronic interaction may be expected in the final states, and these effects may contribute to the breadth of the observed band. The remaining calculated states are out of the range of the photon energies employed in the experiment.

Dyson orbitals for the first two electron detachment energies consist of 2p orbitals that are parallel to the nuclear plane on the two terminal, exocyclic oxygens in antisymmetric (b_2) or symmetric (a_1) combination. (See Figure 4.) Contributions from functions on other nuclei are negligible. The next two Dyson orbitals are similarly concentrated on the exocyclic oxygens, but the 2p orbital constituents are perpendicular to the nuclear plane. For the fifth and sixth final states, the dominant functions are still on the same nuclei, but the chief components are 2p orbitals that are aligned with the nearby Al–O bond axes. These results indicate that electron detachments occur with greatest ease from the oxygens with the lowest coordination number. Six electron pairs are in this category. Dyson orbitals pertaining

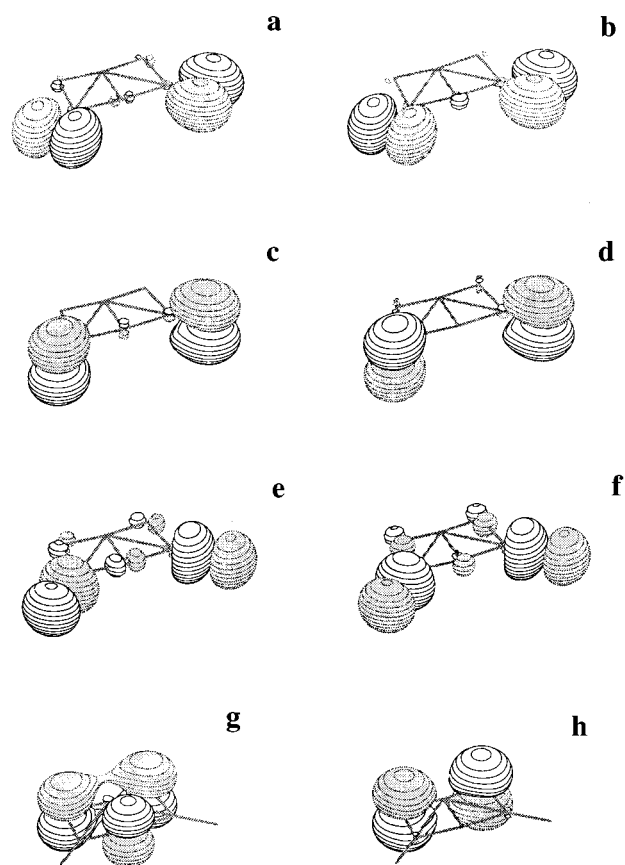


Figure 4. Dyson orbitals for VEDEs of Al_3O_5^- : (a) $^1\text{A}_1 \rightarrow ^2\text{B}_2$, (b) $^1\text{A}_1 \rightarrow ^2\text{A}_1$, (c) $^1\text{A}_1 \rightarrow ^2\text{B}_1$, (d) $^1\text{A}_1 \rightarrow ^2\text{A}_2$, (e) $^1\text{A}_1 \rightarrow ^2\text{B}_2$, (f) $^1\text{A}_1 \rightarrow ^2\text{A}_1$.

to the next few final states are, in general, delocalized over the three remaining oxygens.

Nayak and Nooijen performed similarity-transformed, equation-of-motion calculations on a nonplanar, C_{2v} Al_3O_5^- isomer with two oxygens above and below the plane of the remaining nuclei¹² that resembles the structure of the lower right corner of Figure 1. Examination of this isomer with DF optimizations reveals that it is considerably higher in energy than the lowest C_{2v} structure considered here.

Conclusions

Density functional optimizations and electron propagator calculations have produced accurate, vertical electron detachment energies in close agreement with the photoelectron spectrum of AlO_2^- . Dyson orbitals are, as expected, dominated by oxygen 2p contributions for the $^2\Pi_g$, $^2\Pi_u$, and $^2\Sigma_u$ final states.

DF geometry optimizations indicate the lowest structure of Al_3O_5^- has three, tricoordinate aluminums, three bridging oxygens, and two terminal oxygens. The next most stable structures are planar, but they are not close in energy to the lowest isomer. Three-dimensional structures are even higher in energy. It is likely that the photoelectron spectrum of Al_3O_5^- pertains only to the isomer of lowest energy.

Electron propagator calculations account for the breadth of the peak in the photoelectron spectrum, for there are four final states within 0.2 eV of each other. Dyson orbitals pertaining to these final states, and to two additional states at higher energies, consist chiefly of oxygen 2p functions on the two terminal oxygens.

Acknowledgment. This work was supported by the National Science Foundation under Grant CHE-9873897, by the Kansas DEPSCoR program, by CONACyT and DGAPA, UNAM. Dirección General de Computó Académico at UNAM is acknowledged for providing computer time. We thank Dr. Marcel Nooijen of Princeton University for a preprint of ref 12.

References and Notes

- (1) Desai, S. R.; Wu, H.; Wang, L.-S. *Int. J. Mass Spectrom. Ion Processes* **1996**, *159*, 75.
- (2) Desai, S. R.; Wu, H.; Rohlfing, C. M.; Wang, L.-S. *J. Chem. Phys.* **1997**, *106*, 1309.
- (3) Wu, H.; Li, X.; Wang, X.-B.; Ding, C.-F.; Wang, L.-S. *J. Chem. Phys.* **1998**, *109*, 449.
- (4) Frisch, M. J.; Trucks, G. W.; Schlegel, H. B.; Scuseria, G. E.; Robb, M. A.; Cheeseman, J. R.; Zakrzewski, V. G.; Montgomery, Jr., J. A.; Stratmann, R. E.; Burant, J. C.; Dapprich, S.; Millam, J. M.; Daniels, A. D.; Kudin, K. N.; Strain, M. C.; Farkas, O.; Tomasi, J.; Barone, V.; Cossi, M.; Cammi, R.; Mennucci, B.; Pomelli, C.; Adamo, C.; Clifford, S.; Ochterski, J.; Peterson, G. A.; Ayala, P. Y.; Cui, Q.; Morokuma, K.; Malick, D. K.; Rabuck, A. D.; Raghavachari, K.; Foresman, J. B.; Cioslowski, J.; Ortiz, J. V.; Stefanov, B. B.; Liu, G.; Liashenko, A.; Piskorz, P.; Komaromi, I.; Gomperts, R.; Martin, R. L.; Fox, D. J.; Keith, T.; Al-Laham, M. A.; Peng, C. Y.; Nanayakkara, A.; Gonzalez, C.; Challacombe, M.; Gill, P. M. W.; Johnson, B.; Chen, W.; Wong, M. W.; Andres, J. L.; Head-Gordon, M.; Replogle, E. S.; Pople, J. A. GAUSSIAN 98 (Revision A8); Gaussian, Inc., Pittsburgh, PA, 1998.
- (5) (a) Becke, A. D. *J. Chem. Phys.* **1993**, *98*, 5648. (b) Lee, C.; Yang, W.; Parr, R. G. *Phys. Rev. B* **1988**, *37*, 785.
- (6) (a) Krishnan, R.; Binkley, J. S.; Seeger, R.; Pople, J. A. *J. Chem. Phys.* **1980**, *72*, 650. (b) Clark, T.; Chandrasekhar, J.; Spitznagel, G. W.; Schleyer, P. v. R. *J. Comput. Chem.* **1983**, *4*, 294. (c) Frisch, M. J.; Pople, J. A.; Binkley, J. S. *J. Chem. Phys.* **1984**, *80*, 3265. (d) McLean, A. D.; Chandler, G. S. *J. Chem. Phys.* **1980**, *72*, 5639.
- (7) Pople, J. A.; Head-Gordon, M.; Raghavachari, K. *J. Chem. Phys.* **1987**, *87*, 5968.
- (8) (a) Ortiz, J. V. In *Computational Chemistry: Reviews of Current Trends*; Leszczynski, J., Ed.; World Scientific: Singapore, 1997; Vol. 2, p 1. (b) Ortiz, J. V. *Adv. Quantum Chem.* **1999**, *35*, 33. (c) Ortiz, J. V.; Zakrzewski, V. G.; Dolgounitcheva, O. In *Conceptual Trends in Quantum Chemistry*; Calais, J.-L.; Kryachko, E. S., Eds.; Kluwer: Dordrecht, 1997; Vol. 3, p 465.
- (9) Schaftenaar, G. MOLDEN 3.4, CAOS/CAMM Center, The Netherlands, 1998.
- (10) Ortiz, J. V. *J. Chem. Phys.* **1998**, *108*, 1008.
- (11) (a) Ortiz, J. V. *Chem. Phys. Lett.* **1998**, *296*, 494. (b) Ortiz, J. V. *Chem. Phys. Lett.* **1998**, *297*, 193.
- (12) Nayak, S. K.; Nooijen, M., private communication.